Radiation Measurements 59 (2013) 84–93

Contents lists available at SciVerse ScienceDirect

Radiation Measurements

journal homepage: www.elsevier.com/locate/radmeas

Area radiation monitoring on ISS Increments 17 to 22 using PADLES in the Japanese Experiment Module Kibo

A. Nagamatsu [a,*], K. Murakami [a], K. Kitajo [b], K. Shimada [b], H. Kumagai [b], H. Tawara [a,c]

[a] Japan Aerospace Exploration Agency (JAXA), 2-1-1 Sengen, Tsukuba City, Ibaraki 305-8505, Japan
[b] Advanced Engineering Services, Co. Ltd, 1-6-1 Takezono, Tsukuba City, Ibaraki 305-0032, Japan
[c] High Energy Accelerator Research Organization (KEK), 1-1 Oho, Tsukuba City, Ibaraki 305-0801, Japan

HIGHLIGHTS

- This article shows the first results of dose measurement inside the Japanese Experiment Module Kibo with the PADLES system.
- Generating spatial dose distribution data with the PADLES system are key inputs for benchmarking radiation transport codes.
- For the first time the directional dependence of particle fluence was measured inside the Japanese Experiment Module Kibo.

ARTICLE INFO

Article history:
Received 28 May 2012
Received in revised form
11 March 2013
Accepted 29 May 2013

Keywords:
Area PADLES
Exp PADLES
International Space Station (ISS)
Japanese Experiment Module Kibo
Space radiation dosimetry
CR-39 PNTD
TLD

ABSTRACT

The measurement of radiation environmental parameters in space is essential to support radiation risk assessments for astronauts and establish a benchmark for space radiation models for present and future human space activities. The Japan Aerospace Exploration Agency (JAXA) is performing a continuous area radiation monitoring experiment using the "PAssive Dosimeters for Lifescience Experiments in Space" (PADLES) system inside the Japanese Experiment Module Kibo on board the International Space Station (ISS). The PADLES dosimeter consists of thermoluminescent dosimeters (TLDs) and CR-39 plastic nuclear track detectors (PNTDs). JAXA has run the Area PADLES experiment since the Kibo module was attached to the ISS in June 2008, using 17 dosimeters in fixed locations on the Pressurized Module (PM) and the Experiment Logistics Module-Pressurized Section (ELM-PS) of Kibo, which are replaced every 6 months or every Increment, respectively. For three monitoring periods, known as Area PADLES experiment series #1 to #3, of 301, 180, and 232 days in June 2008 to April 2010 over ISS Increments 17 to 22, the average absorbed dose (dose equivalent) rates of 12 positions in the PM of Kibo were 319 ± 30 μGy/day (618 ± 102 μSv/day), 276 ± 30 μGy/day (608 ± 94 μSv/day), and 293 ± 33 μGy/day (588 ± 84 μSv/day), respectively. The radiation measurement in the ELM-PS was conducted in only Area PADLES experiment series #3 from August 2009 to April 2010 (232 days) over ISS Increments 21 to 22, the average absorbed dose (dose equivalent) rates of 5 positions was 297 ± 28 μGy/day (661 ± 65 μSv/day). The directional dependence of the radiation field was also investigated by installing PADLES dosimeters located in the zenith of ELM-PS of Kibo.

1. Introduction

Radiation measurements performed with active and passive radiation detectors within and outside the International Space Station (ISS) are vital to assess the reliability of current crew dose management procedures and investigate the biological effects of exposure. The National Council on Radiation Protection and Measurements has emphasized the importance of continuous area radiation monitoring in an operational radiation safety program for astronauts working in Low Earth Orbit (LEO) (NCRP, 2002).

The characteristics of LEO space radiation fields have been thoroughly reviewed (Benton and Benton, 2001; NCRP, 2000, 2002). There are three primary radiation sources (galactic cosmic rays ranging from protons to iron, solar particle events, and protons trapped in the Van Allen Belts) in free space outside a spacecraft in LEO at an altitude of 300–500 km. These combine to produce a radiation environment in and around the ISS that depends in a complex way on the solar cycle, the ISS altitude and local shielding due to the ISS structure.

* Corresponding author.
E-mail address: nagamatsu.aiko@jaxa.jp (A. Nagamatsu).

1350-4487/$ – see front matter © 2013 Elsevier Ltd. All rights reserved.
http://dx.doi.org/10.1016/j.radmeas.2013.05.008

Currently there are various types of active detectors and spectrometers: TEPC (Badhwar et al., 1994), IV-TEPC (Semones, 2011) and Medipix (Pinsky et al., 2011) provided by NASA; DB-8, R-16 (Benghin, 2008; Lishnevksii et al., 2010), BTN-M2 (http://l503.iki.rssi.ru/BTNm2-en.html), and Liulin (Dachev et al., 2011; Semkova et al., 2012) by IBMP; DOSTEL (Reitz et al., 2005) by DLR; ALTEA (Di Fino et al., 2011; Narici et al., 2012) by INFN. There are also passive detectors: RAM/APD/CPD (Zhou et al., 2007, 2008) provided by NASA; ID-3 (Petrov, 1997) by IBMP, EuCPD (Straube et al., 2010) by ESA/DLR; HRD-PILLE (Apáthy et al., 2007) by KFKI; RaDI-N (Machrafi et al., 2009) by CSA for neutron doses; and a combination of TLD and CR-39 detectors (Ambrožová et al., 2011). All these detectors measure absorbed doses. Some can also measure dose equivalents based on the relation between the quality factor (Q) and the Linear Energy Transfer (LET) as given in ICRP 60 (ICRP, 1991).

Doke et al. (1995) have proposed a method for space radiation dosimetry using a combination of thermoluminescent dosimeters (TLDs) and CR-39 plastic nuclear track detectors (PNTDs). On the basis of their method, we developed the PAssive Dosimeter for Lifescience Experiments in Space (PADLES), an analysis system that includes a high-speed and high-precision scanning system for acquiring digital images of nuclear tracks on the surface of CR-39 PNTDs and two programs, TLDPADLES and AutoPADLES, to acquire dosimetric results semi-automatically (Nagamatsu et al., 2006, 2009a).

We conducted a series of continuous area radiation monitoring experiments on the ISS inside the Japanese Experiment Module Kibo with PADLES dosimeters. The "Area PADLES" experiments started on 1 June 2008 during Increment 17 just after the attachment of the Japanese Pressurized Module (JPM) to the ISS. Up to now, only Area PADLES dosimeters have been employed for continuous area monitoring since the Kibo module operation got underway. This experiment was part of the Kibo utilization experiment (http://www.nasa.gov/mission_pages/station/research/experiments/Area_PADLES.html). As part of medical equipment operations for crew dose management, NASA RAM, TEPC, and RaDI-N detectors have also been installed on Kibo as the need arose.

We also investigated the directionality of space radiation doses through another experiment called "Exp PADLES". In this paper, we describe the results of area radiation monitoring on board Kibo obtained from the Area PADLES and Exp PADLES experiments from June 2008 to April 2010 (ISS Increments 17–22) (Nagamatsu et al., 2009b, 2010 and 2011a,b).

2. Experiment

2.1. Experiment timeline

The Kibo module mainly consists of a Pressurized Module (PM), the Experiment Logistics Module-Pressurized Section (ELM-PS), and an Exposed Facility (EF). The PM was launched on 1 June 2008. The ELM-PS was launched on 11 March 2008 and relocated on the zenith of the PM after the PM was attached to the ISS in June 2008. The EF was launched on 15 July 2009. Area radiation monitoring had already started when the PM was attached to the ISS in June 2008.

The flight conditions of the Area PADLES (Fig. 1) dosimeters and the Exp PADLES dosimeters (Fig. 2) are summarized in Table 1. The Area PADLES dosimeters were replaced in accordance with the space shuttle flight schedule as shown in Table 1. For all the flight packages at their respective monitoring locations, the installation duration was greater than or equal to 90% of the total flight time, to guarantee the accuracy of the fixed area radiation monitoring.

The Area PADLES series #1 measurements (12 points in the PM) were conducted during ISS Increments 17 and 18. The Area PADLES #2 measurements (12 points in the PM) were conducted from the end of ISS Increment 18 to the end of Increment 20. The Area PADLES #3 measurements (12 points in the PM and 5 points in the ELM-PS) as well as Exp PADLES measurements in the ELM-PS were conducted during ISS Increment 20 and 22.

The experiments were conducted at 12 points in the PM (four starboard and port corners, four close out panels on stand-off in the midsection) and at five points in the ELM-PS (binding site between PM and ELM-PS, the Zenith), as shown in Figs. 3 and 4. At each monitoring point, one PADLES dosimeter was directly attached to the inside wall of Kibo. The body of Exp PADLES (See Fig. 2) was located 19 cm below area monitoring point 17 on the zenith of the ELM-PS during the Area PADLES #3 monitoring period.

As shown in Fig. 4 and Table 2, the surfaces of CR-39 PNTDs at monitoring points 6 and 17 of Area PADLES, and packages 1 and 3 of Exp PADLES were parallel to Earth. Other packages, except for those at points 5, 7, and 8, were kept perpendicular to Earth on the Kibo wall.

The effective shielding thickness averaged over the PM structure and its contents, including racks, increased from 9.7 for Area PADLES #1–15.1 g/cm^2 (water equivalent) for Area PADLES #3 in conjunction with the construction phases of Kibo and because of an increasing number of racks inside the PM.

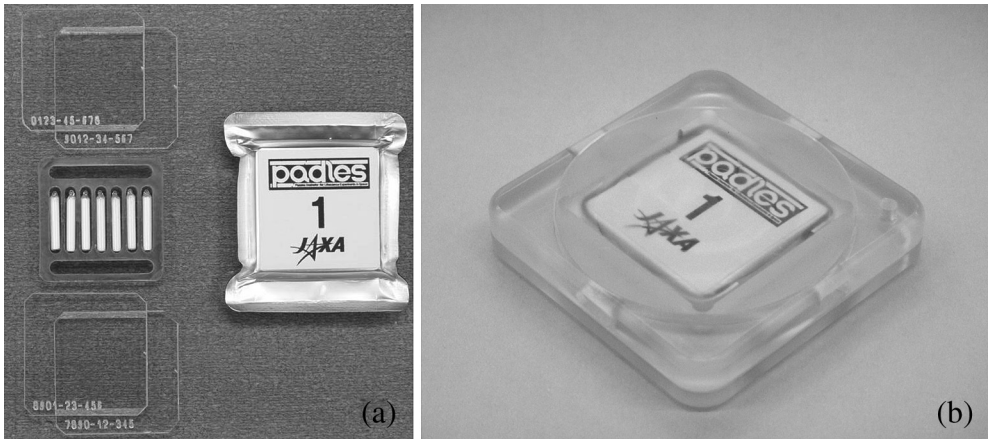

Fig. 1. Pictures of an Area PADLES dosimeter. (a) Four CR-39 PNTDs and seven TLDs installed in an acrylic resin holder (left side). The dosimeter is sealed in an aluminized polyethylene bag (right side). (b) An Area PADLES dosimeter contained in a polycarbonate case.

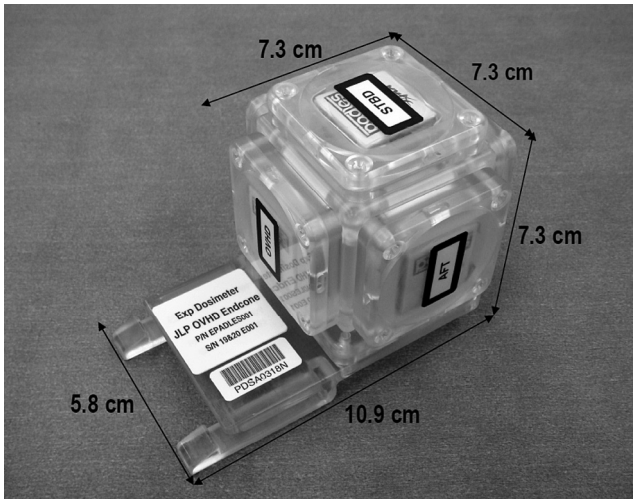

Fig. 2. Picture of the Exp PADLES.

These experiments were executed during the solar minimum at the end of the 23rd to the beginning of the 24th solar cycle. As the 23/24 solar minimum was deeper than the previous three minima (Jian et al., 2011), the fluxes of trapped protons in the South Atlantic Anomaly and galactic cosmic rays were expected to be high. However, in contrast to the effects of solar activity, trapped proton flux decreases with decreasing altitude; the ISS altitudes (Table 1) were lower than those of past flight experiments on space shuttles and on the Mir space station.

2.2. PADLES packages

The PADLES packages were assembled in the JAXA Tsukuba Space Center (JAXA-TKSC) before each flight. A set of flight and ground-control packages were transferred together to the NASA Johnson Space Center (NASA-JSC), whereupon only the flight packages were transferred to a launch pad at the NASA Kennedy Space Center. The ground-control packages were kept at room temperature in a JAXA liaison office in Houston close to the NASA-JSC while the flight packages were in space.

The PADLES packages consisted of two pairs of CR-39 PNTDs (Fukuvi chemical; HARZLAS TD-1) doped with 0.01% of the antioxidant Naugard 445 (Benton et al., 1986; Doke et al., 1988) and seven TLDs (Kyokko; MSO-S) consisting of Mg_2SiO_4:Tb powder sealed in a Pyrex glass tube, as shown on the left side of Fig. 1(a). A reference plate, pre-irradiated with 390 MeV/n C ions and 427 MeV/n Fe ions from the NIRS HIMAC (Heavy Ion Medical Accelerator in Chiba) accelerator in Japan, was also included as part of the CR-39 PNTDs in both the Area and Exp PADLES packages. This was used to check the stability of the track formation sensitivity of the CR-39 PNTDs by comparing with previous values and past flight experiments.

The TLD and CR-39 detectors were hermetically sealed in an aluminized polyethylene bag with air to exclude contact with external gases, such as excess water vapor, and to shield them from light (see the right side of Fig. 1(a)). The bag was placed into a polycarbonate container (4.6 × 4.6 × 0.9 cm) to prevent damage from crew kick load, as shown in Fig. 1(b). Dosimeters for Area PADLES experiments were tethered using Velcro tape to the wall surface inside Kibo.

Fig. 2 shows the body of the unit for the Exp PADLES experiment. This was used to investigate the directional dependence of radiation doses relative to Earth and consisted of Area PADLES dosimeters attached to the six sides of the Exp PADLES cube.

2.3. Dose calculations

After recovery by space shuttle, the flight and ground-control packages were immediately transferred to JAXA-TKSC via NASA-JSC. These packages were then disassembled at JAXA-TKSC, whereupon the TLDs and CR-39 PNTDs were analyzed.

To minimize the PADLES analysis time, two programs have been developed: TLDPADLES used to manage a database of all TLD elements and AutoPADLES for calculating LET distributions to provide absorbed doses and dose equivalents (Nagamatsu et al., 2006, 2009a).

The TLDs' thermoluminescence yields were measured with a TLD reader (Kyokko; TLD reader 2500) from 30 to 400 °C for ~15 s, which was calibrated by exposure to 155 MeV protons from the HIMAC accelerator at NIRS in Japan. Every TLD element was exposed to gamma rays from ^{60}Co to check the individual TL response, and then calibrated based on the sensitivity of the ratio between 155 MeV protons from the HIMAC accelerator and gamma rays from ^{60}Co. TLDPADLES manages a database of all TLD elements held by JAXA, including serial number, history of use, present

Table 1
Flight conditions of Area PADLES and Exp PADLES.

Period No.	Experiment/Monitoring location	Task on board/Vehicle (mission)	Date	Flight time (installation time[d]) [days]	ISS altitude[e] (average) [km]	ISS orbital inclination [deg.]
#1	Area PADLES/PM[a]	Launch/SS[c] (STS-124)	June 1, 2008	301 (278)	339–359 (352)	51.6
		Installation/ISS Kibo	June 12, 2008			
		Retrieval/ISS Kibo	March 17, 2009			
		Return/SS[c] (STS-119)	March 29, 2009			
#2	Area PADLES/PM[a]	Launch/SS[c] (STS-119)	March 16, 2009	180 (164)	343–355 (350)	51.6
		Installation/ISS Kibo	March 19, 2009			
		Retrieval/ISS Kibo	August 30, 2009			
		Return/SS[c] (STS-128)	September 12, 2009			
#3	Area PADLES/PM[a] & ELM-PS[b]	Launch/SS[c] (STS-128)	August 29, 2009	232 (214)	337–350 (343)	51.6
	Exp PADLES/ELM-PS[b]	Installation/ISS Kibo	September 14, 2009			
		Retrieval/ISS Kibo	April 16, 2010			
		Return/SS[c] (STS-131)	April 18, 2010			

[a] Kibo's Pressurized Module.
[b] Kibo's Experiment Logistics Module – Pressurized Section.
[c] NASA's Space Shuttle.
[d] Installation time of the Area PADLES dosimeters and the Exp PADLES dosimeter at measurement points for area monitoring in the Kibo module.
[e] ISS altitude data was provided from Celes Track by private communication.

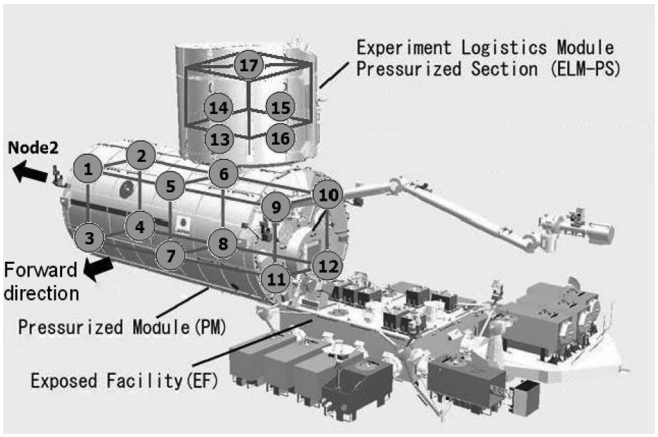

Fig. 3. Kibo as of 2010. The circled numbers show the monitoring points with Area PADLES dosimeters.

status, individual calibration constants for protons and ^{60}Co gamma rays, and TL readouts in past exposure experiments. By using TLDPADLES, a set of TLD elements was selected for each flight experiment to ensure a response deviation of less than 3%.

The TLD data were corrected for long-term fading at room temperature from annealing to read-out via a flight experiment. The fading correction factor was estimated considering annealing and launch date, the flight duration and the storage time from return to measurement at room temperature (Nagamatsu et al., 2011a,b; Tawara et al., 2011). We also confirmed the absence of a fading effect in the CR-39 PNTDs during the long-term experiments using the reference plate that was pre-irradiated with C and Fe ions.

Two pieces of the CR-39 PNTD in each PADLES package were etched in a 7 N NaOH solution at 70 °C. The etching time was 5.5 h for short range particles (SRP) and 13.5 h for long-range particles (LRP). The etched surfaces of each plate were automatically scanned with a high-speed and high-precision scanning system to acquire digital images (Lusex-SE, NIREKO and HSP-1000, SEIKO). The major and minor axes of the surface ellipses of each track were automatically measured using the AutoPADLES program developed by JAXA and incorporating an ellipse-fitting algorithm (Yasuda et al., 2005) to select up to 1000 conically etched tracks per plate. The AutoPADLES program can quickly process numerous digital images of nuclear tracks acquired by the scanning system. Track formation sensitivity was calculated using the major and minor axes and the bulk etch amount (thickness removed by chemical etching from the pre-etched surface of a CR-39 PNTD). Calibration curves have been obtained with HIMAC for heavy ions perpendicularly incident on TD-1 plates. Since the sensitivity of track formation for the CR-39 PNTDs is dependent on dip angle, especially for lower-LET heavy ions, we obtained LET distributions to take into account the dip angle dependence in track formation sensitivity of the antioxidant-doped CR-39 PNTDs, whereby the space radiation field is assumed to be isotropic. In the present analysis method, the CR-39 PNTDs measured space radiation particles incident at the surfaces with dip angles between 80° and 90° over a LET region from 10 to 50 keV/μm for SRP and those with dip angles between 60° and 90° over the LET region of 50 keV/μm and greater for LRP (Tawara et al., 2008). Total LET distributions were ultimately obtained by combining the LET distributions for above and below 50 keV/μm.

The CR-39 PNTDs can practically measure space radiation fluences as a function of LET, L, in the LET region above 2.8 keV/μm (Ogura et al., 2001). Conversely, the detection efficiency of TLDs starts decreasing at around 10 keV/μm, thereby measuring only the low LET component of the space radiation field correctly (Doke et al., 1995; Shiragai et al., 1998; Yasuda and Fujitaka, 2000). The total absorbed dose, D_{TOTAL}, the total dose equivalent, H_{TOTAL}, and the mean quality factor, Q_{MEAN}, can be calculated by a combination of CR-39 PNTD data and TLD data as follows (Doke et al., 1995):

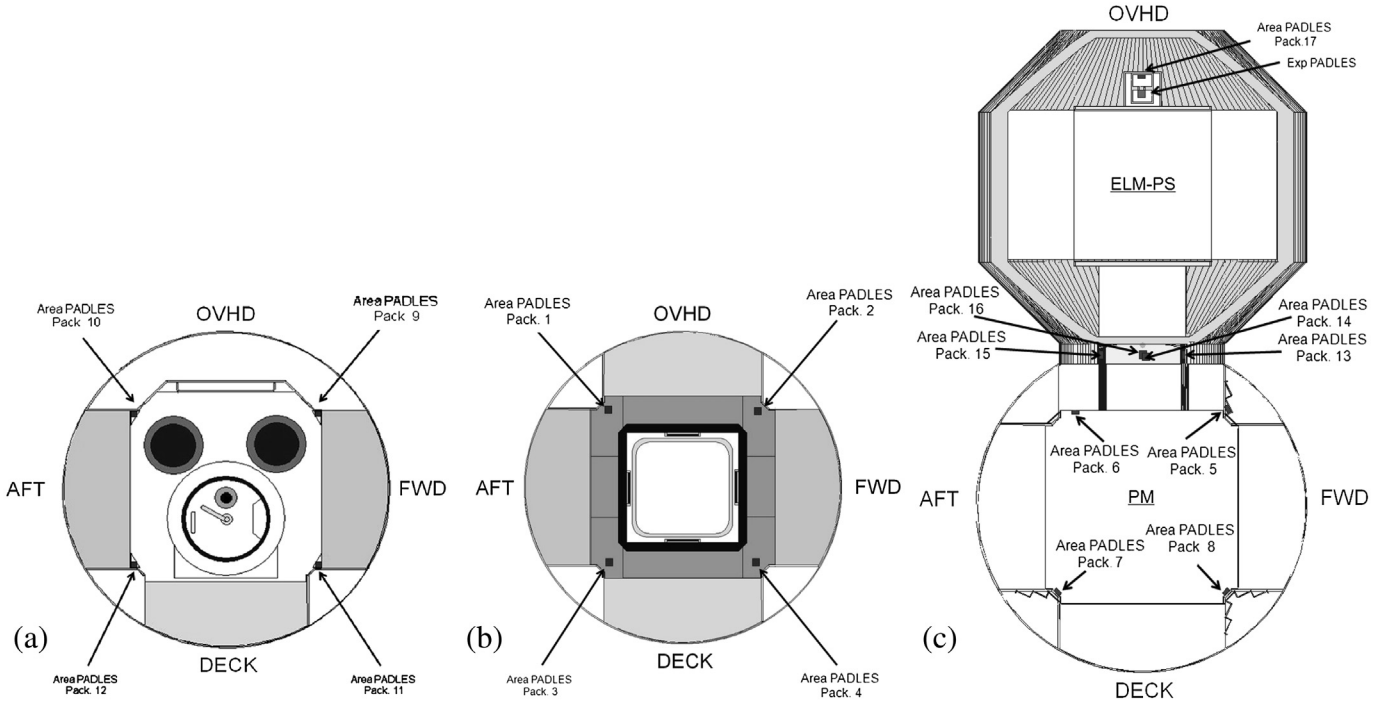

Fig. 4. Location of Area PADLES and Exp PADLES dosimeters in a cross-sectional view of Kibo. (a) The port side of PM, having an air lock. (b) The starboard side of PM. (c) Cross-sectional view of PM and ELM-PS from the starboard side perspective.

Table 2
Installation conditions of the Exp PADLES dosimeters.

Package No.	Direction in ELM-PS	Orientation relative to Earth[a]
1	Bottom	Parallel
2	Aft	Perpendicular
3	Zenith	Parallel
4	Forward	Perpendicular
5	Port	Perpendicular
6	Starboard	Perpendicular

[a] Orientation of the surfaces of CR-39 PNTDs in each Exp PADLES dosimeter relative to Earth.

$$D_{TOTAL} = D_{<Lth} + D_{\geq Lth} = (D_{TLD} - \kappa D_{CR-39}) + D_{CR-39} = D_{TLD} + (1-\kappa)D_{CR-39} \quad (\text{mGy} - \text{water}). \tag{1}$$

$$H_{TOTAL} = D_{<Lth} + H_{\geq Lth} = (D_{TLD} - \kappa D_{CR-39}) + H_{CR-39}(\text{mSv}). \tag{2}$$

$$Q_{MEAN} = H_{TOTAL}/D_{TOTAL}. \tag{3}$$

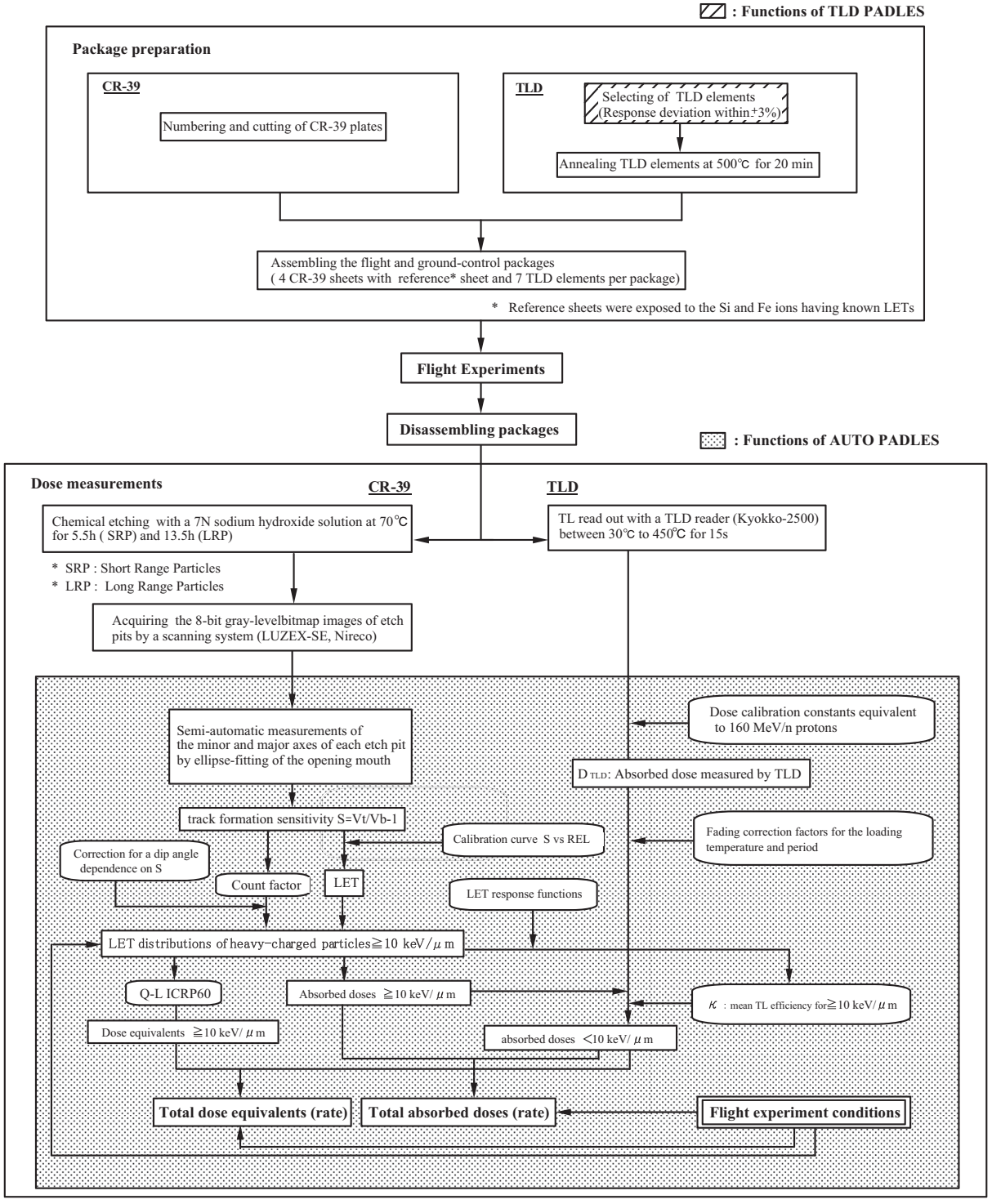

Fig. 5. Standard space radiation dosimetry procedure for PADLES. This figure was modified from a figure in a previous publication (Nagamatsu et al., 2006).

Since the quality factor Q is unified below 10 keV/μm in the Q-L relation of ICRP 60 (ICRP, 1991), we set L_{th} = 10 keV/μm in the present calculation. $D_{CR\text{-}39}$ is calculated from the LET distribution in the LET region of 10 keV/μm or greater as measured with CR-39 PNTDs. D_{TLD} is the water-equivalent absorbed dose measured with TLDs. D_{TLD} includes the contribution in the LET region of 10 keV/μm or greater where the thermoluminescent response declines with increasing LET. The parameter κ is the effective reduction factor of the TLD response above L_{th} (=10 keV/μm here):

$$\kappa = \frac{\Sigma_{>Lth}(f(L_c)\Delta D(L_c))}{D_{CR-39}}, \quad (4)$$

where f (L_c) is a relative TL response as a function of LET (Nagamatsu et al., 2006; Tawara et al., 2011) and ΔD (L_c) is the dose absorbed in the LET bin centered on L_c.

AutoPADLES performs automatic calculations of LET distributions, absorbed doses and dose equivalents by combining the TLD and CR-39 PNTD data using Equation (1). The standard procedure for space radiation dosimetry by PADLES is outlined in Fig. 5 (Nagamatsu et al., 2006). The detailed characteristics and analytical procedures of CR-39 PNTDs and the TLDs in PADLES have been described in previous papers (Nagamatsu et al., 2006, 2009a, 2011a,b, Tawara et al., 2008, 2011).

3. Results and discussion

3.1. Error estimates

In addition to statistical error, we can identify several systematic error sources (and give percentages) for space radiation dose measurements with PADLES dosimeters by considering the experimental results obtained to date: the TLD fading correction at room temperature for D_{TLD} (1.1%); the TLD calibration constant for D_{TLD} (2.1%); κ in Eq. (4) (12%); the individual error in the measurement of etch pit sizes of CR-39 PNTDs and the calibration curves of CR-39 PNTDs for $D_{CR\text{-}39}$ and $H_{CR\text{-}39}$ (15.4%); and the ratio of installation time to total flight time for D_{TLD}, $D_{CR\text{-}39}$, and $H_{CR\text{-}39}$ (2%). We include these systematic errors in the dosimetry results.

3.2. Area monitoring with area PADLES

Fig. 6 shows LET distributions using averaged values obtained from 12 area radiation points in PM and five area radiation points in ELM-PS for Area PADLES #1, #2, and #3. LET distributions measured with the Real-Time Radiation Monitoring Device III (RRMD-III) during space shuttle missions STS-84 (May 1997) and STS-91 (June 1998) (Doke et al., 2001) are shown for comparison. The flight conditions of the RRMD-III resembled those during the period of the Area PADLES experiment. The orbital inclination angle was 51.6° and the flight occurred near the solar minimum at the end of the 22nd solar cycle. The average altitude at which the RRMD-III was active was 395 km (379–412 km) in STS-84 and 380 km (370–397 km) in STS-91. In STS-84 and STS-91, particle fluxes over 4–200 keV/μm measured with the CR-39 PNTDs were lower than those measured with the RRMD-III by a factor of approximately 2.5 (Tawara et al., 2002). The analysis of CR-39 PNTDs for space radiation dosimetry has recently been improved (Tawara et al., 2008). Since LET distributions exceeding 10 keV/μm obtained from the CR-39 PNTDs of Area PADLES are used for dose calculation, we compared LET distributions over 10–600 keV/μm (RRMD-III had a range up to approximately 600 keV/μm) obtained from Area PADLES #1–3 and RRMD-III in different solar minimums. The differences in averaged total absorbed doses and dose equivalents in the LET region of 10–600 keV/μm between RRMD-III on board STS-84/STS-91 in the 22 solar minimum and Area PADLES #1–3 in the 23 solar minimum are 14% and 35%, respectively. Although the flight environment (ISS or Space shuttle), shielding environment, and solar minima period differed for the RRMD-III and the Area PADLES, the agreement between the LET distributions obtained from the Area PADLES dosimeters and those from the RRMD-III on board the STS-84 and STS-91 missions was good for comparable LET ranges.

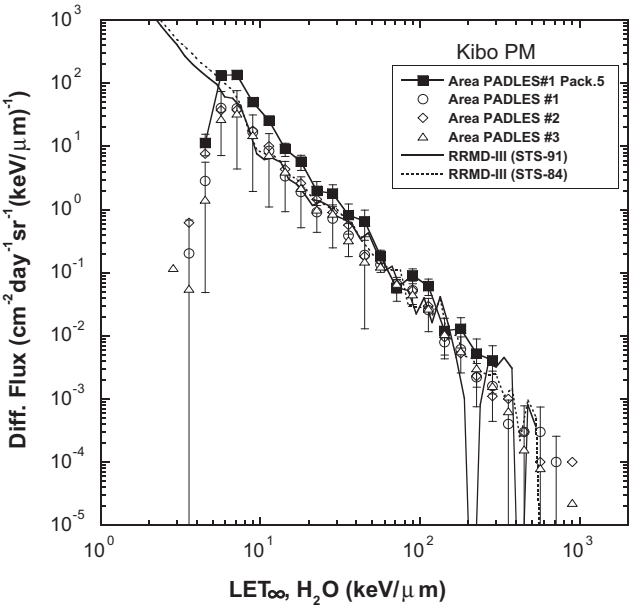

Fig. 6. Averaged LET distributions measured with CR-39 PNTDs located in the Kibo PM. Each error bar indicates the standard deviation of the twelve monitoring points. The LET distributions measured with RRMD-III on board STS-91 and STS-84 (Tawara et al., 2002) are shown for comparison.

Dosimetry results for the PM and ELM-PS are listed in Table 3. The measured values averaged over Area PADLES #1, #2, and #3 were as follows: a D_{TOTAL} rate of 0.220 ± 0.005 to 0.360 ± 0.021 mGy/day, an H_{TOTAL} rate of 0.428 ± 0.026 to 0.877 ± 0.075 mSv/day, and a Q_{MEAN} of 1.61 ± 0.10 to 2.89 ± 0.27.

The D_{TOTAL} rate, H_{TOTAL} rate, and Q_{MEAN} at each monitoring point are plotted in Figs. 7–9, respectively. These figures show that the measurement values fluctuated depending on the monitoring point. The maximum differences between the minimum and maximum values were 50% for the D_{TOTAL} rate (Area PADLES #2), 87% for the H_{TOTAL} rate (Area PADLES #1), and 80% for Q_{MEAN} (Area PADLES #1). We assume the differences in shielding conditions around each monitoring point strongly influenced the measured values. In addition, we note that the fluctuation of the H_{TOTAL} rate far exceeds that of the D_{TOTAL} rate. Another source of fluctuation in the H_{TOTAL} rate might be the installation direction of the CR-39 PNTDs contained in the PADLES dosimeter. We discuss this point in Section 3.3.

Results for position 5 show unique features in Area PADLES #1, #2, and #3 experiments. In Area PADLES #1, position 5 has a $D_{CR\text{-}39}$ dose which exceeds the minimum dose more than fourfold, while the $H_{CR\text{-}39}$ is almost a factor of 3.1 higher than the minimum dose equivalent. In Area PADLES #2 and #3, this feature was also seen. The $Q_{VALUE\_CR\text{-}39}$ for position 5 is around 9.0, 7.5, and 9.3 for Area PADLES #1, #2, and #3, respectively. These values are quite low: in PM, the average value is 11.4. The LET spectrum in Fig. 6 obtained from position 5 for Area PADLES #1 shows that the low LET part of the spectrum is dramatically enhanced. The Area PADLES dosimeter in position 5 was installed on the Z-panel (aluminum, with approximate thickness of less than 3 mm), which is part of the Kibo

Table 3
Results of area radiation monitoring in the Kibo PM and the ELM-PS. Errors are standard deviations.

Program	Monitoring point No.	D_{TLD} rate (mGy/day)	$D_{CR\text{-}39}$ rate > 10 keV/μm (mGy/day)	κ	$H_{CR\text{-}39}$ rate > 10 keV/μm (mSv/day)	D_{TOTAL} rate (mGy/day)	H_{TOTAL} rate (mSv/day)	Q_{MEAN}
Area PADLES #1	1	0.336 ± 0.014	0.0230 ± 0.0022	0.73 ± 0.10	0.285 ± 0.031	0.342 ± 0.014	0.604 ± 0.035	1.77 ± 0.12
	2	0.352 ± 0.021	0.0249 ± 0.0026	0.70 ± 0.10	0.309 ± 0.034	0.360 ± 0.021	0.644 ± 0.040	1.79 ± 0.15
	3	0.241 ± 0.011	0.0186 ± 0.0018	0.72 ± 0.10	0.241 ± 0.026	0.247 ± 0.011	0.470 ± 0.028	1.90 ± 0.14
	4	0.305 ± 0.010	0.0196 ± 0.0021	0.75 ± 0.11	0.209 ± 0.025	0.309 ± 0.010	0.499 ± 0.027	1.61 ± 0.10
	5	0.289 ± 0.011	0.0715 ± 0.0068	0.80 ± 0.11	0.645 ± 0.073	0.303 ± 0.011	0.877 ± 0.075	2.89 ± 0.27
	6	0.320 ± 0.025	0.0235 ± 0.0023	0.74 ± 0.10	0.271 ± 0.029	0.326 ± 0.025	0.573 ± 0.039	1.76 ± 0.18
	7	0.300 ± 0.010	0.0375 ± 0.0039	0.80 ± 0.12	0.331 ± 0.041	0.307 ± 0.010	0.600 ± 0.042	1.95 ± 0.15
	8	0.324 ± 0.011	0.0417 ± 0.0044	0.83 ± 0.12	0.323 ± 0.042	0.331 ± 0.011	0.612 ± 0.044	1.85 ± 0.15
	9	0.287 ± 0.010	0.0246 ± 0.0024	0.71 ± 0.10	0.314 ± 0.034	0.294 ± 0.010	0.583 ± 0.036	1.98 ± 0.14
	10	0.337 ± 0.028	0.0293 ± 0.0031	0.74 ± 0.11	0.335 ± 0.040	0.345 ± 0.028	0.651 ± 0.049	1.89 ± 0.21
	11	0.310 ± 0.018	0.0288 ± 0.0029	0.73 ± 0.10	0.332 ± 0.036	0.317 ± 0.018	0.621 ± 0.041	1.96 ± 0.17
	12	0.336 ± 0.017	0.0274 ± 0.0030	0.70 ± 0.11	0.369 ± 0.040	0.344 ± 0.017	0.685 ± 0.044	1.99 ± 0.16
	Average	0.311 ± 0.030	0.0309 ± 0.0145	0.75 ± 0.04	0.330 ± 0.109	0.319 ± 0.030	0.618 ± 0.102	1.95 ± 0.32
	Min/Max	1.46	3.84	1.19	3.09	1.46	1.87	1.80
Area PADLES #2	1	0.266 ± 0.008	0.0239 ± 0.0023	0.76 ± 0.10	0.256 ± 0.028	0.271 ± 0.008	0.504 ± 0.029	1.86 ± 0.12
	2	0.266 ± 0.019	0.0275 ± 0.0025	0.75 ± 0.10	0.303 ± 0.032	0.273 ± 0.019	0.548 ± 0.038	2.01 ± 0.20
	3	0.215 ± 0.005	0.0183 ± 0.0018	0.73 ± 0.11	0.226 ± 0.026	0.220 ± 0.005	0.428 ± 0.026	1.94 ± 0.13
	4	0.265 ± 0.004	0.0280 ± 0.0026	0.73 ± 0.09	0.319 ± 0.034	0.272 ± 0.004	0.564 ± 0.034	2.07 ± 0.13
	5	0.266 ± 0.011	0.0700 ± 0.0058	0.83 ± 0.10	0.523 ± 0.056	0.278 ± 0.011	0.731 ± 0.057	2.63 ± 0.23
	6	0.253 ± 0.011	0.0335 ± 0.0030	0.75 ± 0.09	0.390 ± 0.040	0.262 ± 0.011	0.619 ± 0.041	2.36 ± 0.19
	7	0.238 ± 0.017	0.0430 ± 0.0040	0.79 ± 0.10	0.390 ± 0.044	0.247 ± 0.017	0.594 ± 0.047	2.41 ± 0.25
	8	0.286 ± 0.018	0.0599 ± 0.0052	0.80 ± 0.10	0.524 ± 0.057	0.298 ± 0.018	0.762 ± 0.060	2.56 ± 0.26
	9	0.258 ± 0.010	0.0343 ± 0.0031	0.78 ± 0.10	0.346 ± 0.035	0.266 ± 0.010	0.578 ± 0.037	2.18 ± 0.16
	10	0.320 ± 0.018	0.0360 ± 0.0035	0.76 ± 0.10	0.371 ± 0.042	0.329 ± 0.018	0.664 ± 0.046	2.02 ± 0.18
	11	0.265 ± 0.011	0.0373 ± 0.0040	0.73 ± 0.10	0.387 ± 0.045	0.275 ± 0.011	0.625 ± 0.046	2.27 ± 0.19
	12	0.312 ± 0.024	0.0349 ± 0.0031	0.77 ± 0.10	0.389 ± 0.038	0.320 ± 0.024	0.674 ± 0.045	2.10 ± 0.21
	Average	0.268 ± 0.029	0.0372 ± 0.0147	0.77 ± 0.03	0.369 ± 0.090	0.276 ± 0.030	0.608 ± 0.094	2.20 ± 0.25
	Min/Max	1.49	3.83	1.14	2.32	1.50	1.78	1.41
Area PADLES #3 in PM	1	0.276 ± 0.012	0.0216 ± 0.0021	0.75 ± 0.10	0.256 ± 0.027	0.281 ± 0.012	0.515 ± 0.030	1.83 ± 0.13
	2	0.295 ± 0.019	0.0190 ± 0.0019	0.75 ± 0.10	0.213 ± 0.025	0.300 ± 0.019	0.493 ± 0.031	1.65 ± 0.15
	3	0.236 ± 0.009	0.0228 ± 0.0021	0.74 ± 0.10	0.271 ± 0.029	0.242 ± 0.009	0.490 ± 0.030	2.03 ± 0.15
	4	0.277 ± 0.013	0.0209 ± 0.0020	0.73 ± 0.10	0.242 ± 0.026	0.282 ± 0.013	0.503 ± 0.029	1.78 ± 0.13
	5	0.293 ± 0.009	0.0541 ± 0.0047	0.80 ± 0.10	0.503 ± 0.055	0.304 ± 0.009	0.753 ± 0.056	2.48 ± 0.20
	6	0.296 ± 0.015	0.0285 ± 0.0025	0.75 ± 0.09	0.341 ± 0.033	0.303 ± 0.011	0.616 ± 0.037	2.03 ± 0.16
	7	0.236 ± 0.011	0.0475 ± 0.0041	0.79 ± 0.10	0.425 ± 0.043	0.246 ± 0.011	0.623 ± 0.045	2.54 ± 0.22
	8	0.309 ± 0.009	0.0392 ± 0.0036	0.79 ± 0.10	0.362 ± 0.039	0.318 ± 0.009	0.641 ± 0.040	2.02 ± 0.14
	9	0.259 ± 0.010	0.0233 ± 0.0022	0.76 ± 0.10	0.268 ± 0.030	0.265 ± 0.010	0.510 ± 0.031	1.92 ± 0.14
	10	0.325 ± 0.012	0.0268 ± 0.0025	0.75 ± 0.10	0.325 ± 0.035	0.331 ± 0.012	0.630 ± 0.037	1.90 ± 0.13
	11	0.282 ± 0.008	0.0308 ± 0.0028	0.73 ± 0.09	0.362 ± 0.035	0.290 ± 0.008	0.622 ± 0.036	2.14 ± 0.14
	12	0.347 ± 0.014	0.0360 ± 0.0034	0.77 ± 0.10	0.346 ± 0.037	0.356 ± 0.014	0.666 ± 0.040	1.87 ± 0.14
	Average	0.286 ± 0.033	0.0309 ± 0.0112	0.76 ± 0.02	0.326 ± 0.083	0.293 ± 0.033	0.588 ± 0.084	2.02 ± 0.26
	Min/Max	1.47	2.85	1.10	2.36	1.47	1.54	1.54
Area PADLES #3 in ELM-PS	13	0.295 ± 0.031	0.0400 ± 0.0035	0.79 ± 0.10	0.388 ± 0.040	0.303 ± 0.031	0.651 ± 0.051	2.15 ± 0.28
	14	0.310 ± 0.014	0.0370 ± 0.0033	0.75 ± 0.09	0.409 ± 0.043	0.319 ± 0.014	0.691 ± 0.045	2.17 ± 0.17
	15	0.306 ± 0.023	0.0436 ± 0.0041	0.78 ± 0.11	0.411 ± 0.045	0.315 ± 0.023	0.682 ± 0.051	2.16 ± 0.23
	16	0.290 ± 0.015	0.0414 ± 0.0035	0.77 ± 0.09	0.467 ± 0.046	0.299 ± 0.015	0.725 ± 0.048	2.42 ± 0.20
	17	0.242 ± 0.007	0.0294 ± 0.0025	0.74 ± 0.09	0.335 ± 0.031	0.249 ± 0.007	0.555 ± 0.032	2.22 ± 0.14
	Average	0.289 ± 0.027	0.0383 ± 0.0055	0.77 ± 0.02	0.402 ± 0.048	0.297 ± 0.028	0.661 ± 0.065	2.22 ± 0.11
	Min/Max	1.28	1.48	1.07	1.40	1.28	1.31	1.13

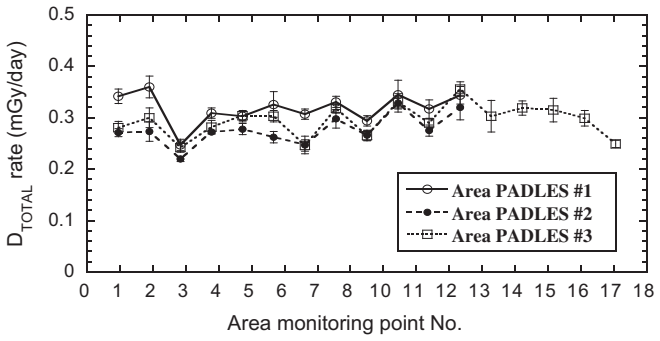

Fig. 7. Total absorbed dose rates in the Kibo PM obtained in Area PADLES #1, #2, and #3.

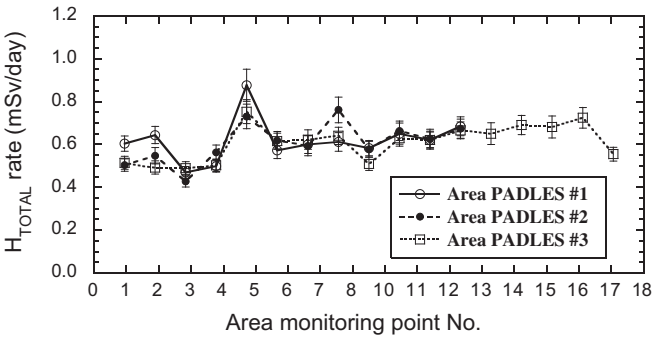

Fig. 8. Total dose equivalent rates in the Kibo PM obtained in Area PADLES #1, #2, and #3.

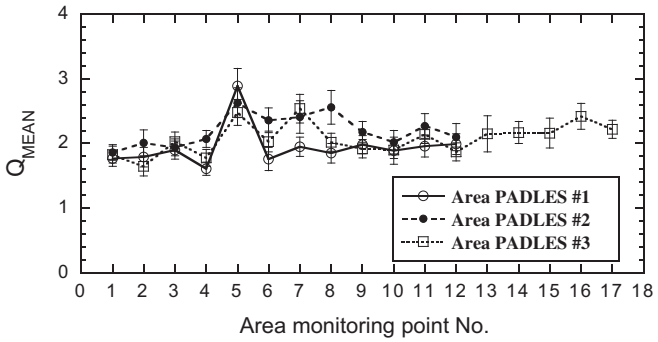

Fig. 9. Mean quality factors in the Kibo PM obtained in Area PADLES #1, #2, and #3.

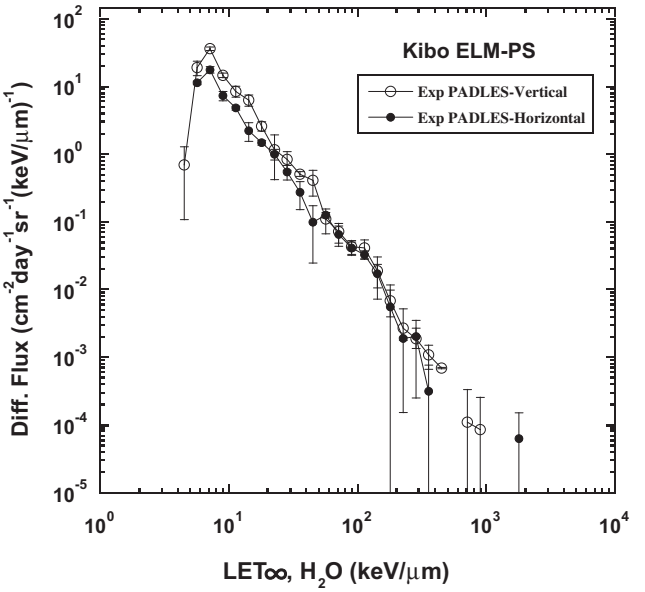

Fig. 10. Averaged LET distributions as measured with CR-39 PNTDs set horizontally and vertically, located in the Exp PADLES unit on the zenith of the Kibo ELM-PM. Error bars indicate the standard deviations of results from the Exp PADLES dosimeter in the same orientation.

structure and is very close to the Kibo body as shown in Fig. 4. From the outer-space perspective, the shielding thickness at position 5 is the thinnest of all the dosimeter positions. Other Area PADLES dosimeters are set on inside walls, with shielding that is thicker than that at position 5. With this in mind, particle fluxes <50 keV/μm in position 5 were up to 4 times the level of averaged particle fluxes obtained from Area PADLES #1 dosimeters in other positions (1–12). Consequently, Q_{MEAN} for position 5 has the highest value for Area PADLES #1 to #3.

NASA RAM dosimeters were also installed at positions 7 and 9 from Increment 18, November 2008 and at position 15 from Increment 29, October 2011. The flight durations of JAXA Area PADLES and NASA RAM varied because each agency used different vehicles for launch and return. Gaza et al. (2010) presented the RAM dosimetry results, including a measurement in Kibo over Increments 18 to 20. Their results show absorbed doses in positions 7 and 9 of approximately 250 and 275 μGy/day. Over the period covered by their results straddles Area PADLES #1 and #2, and the dose values seem to be consistent within error. A further detailed comparison of the dose equivalent is needed using the LET distributions obtained by each CR-39 PNTD.

3.3. Directional dependence measurement with Exp PADLES

Fig. 10 shows a comparison with averaged LET distributions between dosimeters attached horizontally and vertically to the body of the Exp PADLES unit. The horizontal (Parallel in Table 2) LET distributions average the results of package Nos. 1 and 3, while the vertical (Perpendicular in Table 2) LET distributions average the results of package Nos. 2, 3, 4, and 6 (see Table 2).

In the vertical LET distributions the low LET part of the spectrum is enhanced compared to the horizontal LET distributions. LET distributions and particle fluxes from Area PADLES Nos. 6 and 17 (in PM and ELM-PS, respectively), which are oriented parallel to Earth correlate very well with the horizontal LET distribution in Fig. 10. The particle fluxes obtained by CR-39 PNTDs in the horizontally-set packages are approximately half the fluxes obtained from packages installed perpendicularly in ELM-PS.

The dosimetry results for ELM-PS are listed in Table 4. For the Exp PADLES dosimeters set horizontally the average doses are as follows. The $D_{CR\text{-}39}$ rate is 0.026 mGy/day and the $H_{CR\text{-}39}$ rate is 0.316 mSv/day, For the dosimeters set vertically the $D_{CR\text{-}39}$ rate is 0.041 mGy/day and the $H_{CR\text{-}39}$ rate is 0.434 mSv/day. The differences between horizontal and vertical values are 63 and 73% in $D_{CR\text{-}39}$ and $H_{CR\text{-}39}$, respectively.

The $D_{CR\text{-}39}$ and $H_{CR\text{-}39}$ rates for the Exp PADLES dosimeters are plotted in Fig. 11. The $D_{CR\text{-}39}$ and $H_{CR\text{-}39}$ rates of Exp PADLES dosimeters 1 and 3 installed parallel to Earth are lower than those of dosimeters installed perpendicularly. Similar variations of D_{TOTAL} and H_{TOTAL} rates were also obtained from the Area PADLES dosimeters corresponding to the directions of the Exp PADLES dosimeter packages 13 to 17 in ELM-PS.

Exp PADLES has three mutually orthogonal directions: *X* (Starboard, Package 6 − Port, Package 5), *Y* (Forward, Package 4 − Aft, Package 2), *Z* (Zenith, Package 3 − Bottom, Package 1). There were no differences between *X* and *Y* in terms of particle fluxes, $D_{CR\text{-}39}$ or the $H_{CR\text{-}39}$ rate (see Table 4).

Table 4
Results of radiation monitoring using Exp PADLES in the Kibo ELM-PS. Errors are standard deviations.

Program	Package No.	D_{TLD} rate (mGy/day)	$D_{CR\text{-}39}$ rate > 10 keV/μm (mGy/day)	κ	$H_{CR\text{-}39}$ rate > 10 keV/μm (mSv/day)	D_{TOTAL} rate (mGy/day)	H_{TOTAL} rate (mSv/day)	Q_{MEAN}
Exp PADLES	1	0.263 ± 0.010	0.0245 ± 0.0021	0.74 ± 0.09	0.307 ± 0.030	0.269 ± 0.010	0.552 ± 0.032	2.05 ± 0.14
	2	0.270 ± 0.012	0.0419 ± 0.0035	0.78 ± 0.09	0.416 ± 0.042	0.280 ± 0.012	0.653 ± 0.043	2.34 ± 0.19
	3	0.274 ± 0.011	0.0268 ± 0.0029	0.70 ± 0.10	0.325 ± 0.033	0.282 ± 0.011	0.580 ± 0.035	2.06 ± 0.15
	4	0.266 ± 0.014	0.0385 ± 0.0035	0.77 ± 0.10	0.401 ± 0.041	0.275 ± 0.014	0.637 ± 0.044	2.32 ± 0.20
	5	0.284 ± 0.013	0.0430 ± 0.0040	0.74 ± 0.10	0.459 ± 0.048	0.295 ± 0.013	0.711 ± 0.050	2.41 ± 0.20
	6	0.271 ± 0.011	0.0396 ± 0.0035	0.73 ± 0.09	0.458 ± 0.046	0.282 ± 0.011	0.700 ± 0.047	2.49 ± 0.20
	Average	0.271 ± 0.007	0.0357 ± 0.0080	0.74 ± 0.03	0.394 ± 0.065	0.281 ± 0.009	0.639 ± 0.063	2.28 ± 0.18
	Min/Max	1.08	1.76	1.11	1.50	1.10	1.29	1.21

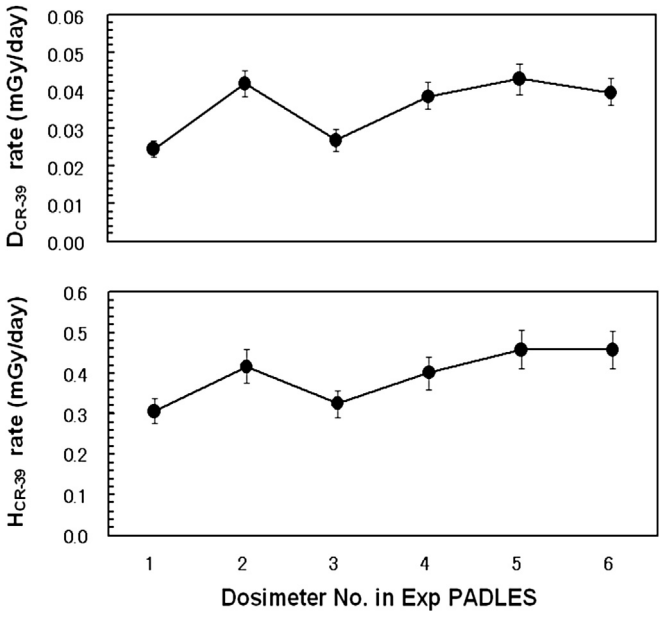

Fig. 11. The D_{CR-39} and H_{CR-39} rates in the Kibo ELM-PS obtained in Exp PADLES. Packages 1 and 3 of Exp PADLES were parallel to Earth. Packages 2, 3, 4, and 6 of Exp PADLES were perpendicular (see Table 2).

Since we measured space radiation particles incident at the surfaces with dip angles between 80° and 90° over an LET region from 10 to 50 keV/μm and those with dip angles between 60° and 90° over the LET region above 50 keV/μm, CR-39 PNTD data show positional and directional sensitivity. We conclude that the Exp PADLES experiment evaluating changes in D_{CR-39} and H_{CR-39} depends on the installation orientation on the ISS Kibo.

Approximately 87% of the D_{TOTAL} rate was measured with the TLDs, which are non-directional dosimeters. The TLDs used in the PADLES dosimeters have a virtually uniform TL response with respect to the incident angle of high-energy long-range protons, meaning the directional dependence is not apparent in total absorbed doses and dose equivalents.

4. Conclusions

We conducted three area radiation monitoring experiments in the Kibo module on the ISS with PADLES dosimeters over the period from 1 June 2008 to 18 April 2010 during a solar minimum.

In the Pressurized Module of Kibo, the absorbed dose rates and the dose equivalent rates from Area PADLES #1 (1 June 2008 to 29 March 2009) were 247–360 μGy/day and 470–877 μSv/day. The corresponding rates from Area PADLES #2 (16 March 2009 to 12 September 2009) were 220–329 μGy/day and 428–762 μSv/day and those from Area PADLES #3 & Exp PADLES (29 August 2009 to 18 April 2010) were 242–356 μGy/day and 490–753 μSv/day, respectively.

We also investigated the dependence of radiation dose on dosimeter installation orientation with a compact Exp PADLES unit in the ELM-PS. It was found that the particle fluxes, DCR_{39} and H_{CR-39} rate changes twice, 1.6 and 1.4 respectively, depending on the installation orientation, because CR-39 PNTDs have a directional response. These differences are attributable to the fact that the rate of increase is high in the low LET part of the spectra, because horizontally-set CR-39 PNTDs are shielded by Earth itself.

This suggests that space radiation fields on the ISS are not isotropic. Di Fino et al. (2011) used an ALTEA spectrometer with a 3D applied detector system to show that GCR flux (LET in silicon $>$ 50 keV/μm) is anisotropic (up to factor 3) inside the ISS due to the shielding configurations. Lower LET regions would also be anisotropic, as shown in Figs. 10 and 11, due to differences in the inner radiation environment and the shielding role of Earth itself. The influence on the angular distributions of space radiation fields of the surrounding shielding conditions and the directionality of radiation sources should therefore be taken into consideration when monitoring radiation in LEO. Detailed knowledge of the radiation environment inside the International Space Station which has uneven shielding is mandatory for an accurate radiation risk assessment.

This continuous area monitoring is used as a benchmark for the space radiation models we have developed. These are constructed based on the Particle and Heavy Ion Transport code System (PHITS) (Iwase et al., 2002) and incorporate a precise description of the Kibo Shielding environment (Nagamatsu et al., 2010). We expect these space radiation models to be useful in risk assessment during interplanetary missions beyond Earth. The results of Area PADLES are the cornerstone of this development. We must focus on the fact that doses during interplanetary missions would certainly exceed those on board the ISS due to GCR contributions from all directions and the absence of a magnetic field. On the surface of the moon or Mars, we must also consider the directionality of radiation sources just as we should for the ISS orbiting Earth.

Acknowledgments

The authors thank Dr. T. S. Kelso and Celes Track for providing continuous ISS attitude data. The authors also acknowledge the help of the following colleagues in realizing the Kibo flight experiments: T. Mizuno and Y. Abiru of the small payload group 'GNOME'; K. Kawada of JET; C. Harada and K. Okada of JEM-Payloads; K. Komatsu of the J-PLAN team; Dr. M. Furukawa of J-POC; and JAXA Increment scientists, payload managers, and all others involved. We sincerely thank the astronauts who conducted our experiments on board Kibo: Dr. G. E. Chamitoff and Dr. S. H. Magnus for Area PADLES #1; Mr. E. M. Fincke and Mr. F. DeWinne, for Area PADLES #2; and Ms. N. P. Stott and Mr. S. Noguchi for Area PADLES #3. Part of this work was carried out under the Research Project with Heavy Ions at NIRS HIMAC (12P095, 12P104, 13P127, and 17P-205).

References

Ambrožová, I., Brabcová, K., Spurný, F., Shurshakov, V.A., Kartsev, I.S., Tolochek, R.V., 2011. Monitoring on board spacecraft by means of passive detectors. Radiat. Prot. Dosimetry. 144 (1–4), 605–610.

Apáthy, I., Akatov, Yu. A., Arkhangelsky, V.V., Bodnár, L., Deme, S., Fehér, I., Kaleri, A., Padalka, I., Pázmándi, T., Reitz, G., Sharipov, S., 2007. TL dose measurements on board the Russian segment of the ISS by the "Pille" system during Expedition-8, -9 and -10. Acta. Astronaut. 60 (4–7), 322–328.

Badhwar, G.D., Cucinotta, F.A., Braby, L.A., Konradi, A., 1994. Measurements on the shuttle of the b LET spectra of galactic cosmic radiation and comparison with the radiation transport model. Radiat. Res. 139, 344–351.

Benghin, V.V., February 2008. On-board predicting algorithm of radiation exposure for the International Space Station radiation monitoring system. Original Res. Article J. Atmos. Solar-terrestrial Phys. 70 (2–4), 675–679.

Benton, E.R., Benton, E.V., 2001. Space radiation dosimetry in low-earth orbit and beyond. Nucl. Instr. Meth. 184, 255–294.

Benton, E.V., Ogura, K., Frank, A.L., Atallah, T.M., Rowe, V., 1986. Response of different types of CR-39 to energetic ions. Nucl. Tracks. Radiat. Meas. 12, 79–82.

Dachev, T.P., Semkova, J., Tomov, B., 2011. Space shuttle drops down the SAA doses on ISS. Adv. Space. Res. 47, 2030–2038.

Di Fino, L., Casolino, M., De Santis, C., Larosa, M., La Tessa, C., Narici, L., Picozza, P., Zaconte, V., 2011. Heavy-Ion Anisotropy measured by ALTEA in the international space station. Radiat. Res. 176 (3), 397–406.

Doke, T., Tawara, H., Hayashi, T., Ichinose, H., Kuwahara, K., Nakamura, S., Orito, S., Ogura, K., 1988. CR-39 plastic for massive magnetic monopole search. Nucl. Instrum. Methods B 34, 81–88.

Doke, T., Hayashi, T., Nagaoka, S., Ogura, K., Takeuchi, R., 1995. Estimation of dose equivalent in STS-47 by a combination of TLDs and CR-39. Radiat. Meas. 24, 75–82.

Doke, T., Hayashi, T., Kikuchi, J., Sakaguchi, T., Terasawa, K., Yoshihira, E., Nagaoka, S., Nakano, T., Takahashi, S., 2001. Measurements of LET-distribution, dose equivalent and quality factor with the RRMD-III on the Space Shuttle Missions STS-84, -89 and -91. Radiat. Meas. 33, 373–387.

Gaza, R., Zhou, D., Roed, Y., Steenburgh, R., Lee, K., Fry, F.D., Semones, E., Reitz, G., Berger, T., O'Sullivan, D., Zapp, N. 2010. ISS Measurements at Solar Minimum (2008–2010). In: The Fifteenth WRMISS Workshop took place on 7–9 September 2010 in Frascati, Italy. http://www.wrmiss.org/workshops/fifteenth/Zapp.pdfhttp://wrmiss.org/workshops/fifteenth/.

ICRP, 1991. Recommendations of the International Commission on Radiological Protection. ICRP Publication 60, Annals of the ICRP 21, Nos. 1–3. Pergamon Press, New York.

Iwase, H., Niita, K., Nakamura, T., 2002. Development of general-purpose particle and heavy ion transport code. J. Nucl. Sci. Technol. 39, 1142.

Jian, L.K., Russell, C.T., Luhmann, J.G., 2011. Comparing solar minimum 23/24 with historical solar wind records at 1 AU. Solar Phys. 274, 321–344.

Lishnevskii, A.E., Panasyuk, M.I., Benghin, V.V., Petrov, V.M., Volkov, A.N., Nechayev, O.Y., 2010. Variations of radiation environment on board the ISS in the year 2008. Cosmic Res. 48 (3), 212–217.

Machrafi, R., Garrow, K., Ing, H., Smith, M.B., Andrews, H.R., Akatov, Yu., Arkhangelsky, V., Chernykh, I., Mitrikas, V., Petrov, V., Shurshakov, V., Tomi, L., Kartsev, I., Lyagushin, V., 2009. Neutron dose study with bubble detectors aboard the International Space Station as part of the Matroshka-R experiment. Radiat. Prot. Dosimetry. 133 (4), 200–207.

Nagamatsu, A., Masukawa, M., Kamigaichi, S., Kumagai, H., Masaki, M., Nakahiro, Y., Yasuda, H., Benton, E., Takayoshi, H., Tawara, H., 2006. Development of the space radiation dosimetry system 'PADLES'. In: 20th Workshop on Radiation Detectors and Their Users, pp. 23–36. http://ccdb5fs.kek.jp/tiff/2006/0627/0627046.pdf.

Nagamatsu, A., Murakami, K., Araki, S., Kumagai, H., Kitajo, K., Tawara, H., 2009a. Space radiation dosimetry in low Earth orbit by a passive and integrating dosimeter – 'PADLES'. In: 22nd Workshop on Radiation Detectors and Their Uses, KEK Proceedings 2008–14, pp. 167–177. http://ccdb5fs.kek.jp/tiff/2008/0825/0825014.pdf.

Nagamatsu, A., Murakami, K., Tawara, H., Kumagai, H., Kitajo, K., 2009b. First area monitoring using area PADLES on board the KIBO. In: The Fourteenth WRMISS Workshop took Place on 8–10 September 2009 in Dublin, the Republic of Ireland. http://wrmiss.org/workshops/fourteenth/.

Nagamatsu, A., Murakami, K., Tawara, H., Kumagai, H., Kitajo, K., 2010. Radiation monitoring using area PADLES on board the ISS Japanese Experiment Module, Kibo. In: The Fifteenth WRMISS Workshop Took Place on 7–9 September 2010 in Frascati, Italy.

Nagamatsu, A., Murakami, Yokota, A., Yamazaki, J., Yamauchi, M., Kumagai, H., Tawara, H., 2011a. Radiation damage to HDTV camera CCDs on board the International Space Station. Radiat. Meas. 46, 205–212.

Nagamatsu, A., Murakami, K., Tawara, H., Kitajo, K., Shimada, K., Kumagai, H., 2011b. Radiation monitoring using PADLES on board the ISS Japanese Experiment Module, Kibo. In: The Sixteenth WRMISS Workshop Took Place on 6–8 September 2011 in Prague, the Czech Republic. http://wrmiss.org/workshops/sixteenth/.

Narici, L., Casolino, M., Di Fino, L., Larosa, M., Larsson, O., Picozza, P., Zaconte, V., 2012. Iron flux inside the International Space Station is measured to be lower than predicted. Radiat. Meas. 47 (10), 1030–1034.

NCRP, 2000. Radiation Protection Guidance for Activities in Low-Earth-Orbit. NCRP Report No. 132.

NCRP, 2002. Operational Radiation Safety Program for Astronauts in Low-earth Orbit: a Basic Framework. NCRP Report No. 142.

Ogura, K., Asano, M., Yasuda, N., Yoshida, M., 2001. Properties of TNF-1 track etch detector. Nucl. Instr.. Meth., B 185, 222–227.

Petrov, V.M., 1997. Present and future radiation dosimetry for Russian cosmonauts. Radiat. Res. 148 (5s), S24–S32.

Pinsky, L., Stoffle, N., Empl, A., Jakubek, J., Pospisil, S., Leroy, C., Kitamura, H., Yasuda, N., Uchihori, Y., 2011. Application of the Medipix2 technology to space radiation dosimetry and hadron therapy beam monitoring. Radiat. Meas. 46 (12), 1610–1614.

Reitz, G., Beaujean, R., Benton, E., Burmeister, S., Dachev, T., Deme, S., Luszik-Bhadra, M., Olko, P., 2005. Space radiation measurements on-board ISS -the DOSMAP experiment. Radiat. Prot. Dosimetry. 116, 374–379.

Semkova, J., Koleva, R., Maltchev, St., Bankov, N., Benghin, V., Chernykh, I., Shurshakov, V., Petrov, V., Drobyshev, S., Nikolaev, I., 2012. Depth dose measurements with the Liulin-5 experiment inside the spherical phantom of the MATROSHKA-R project on board the International Space Station. Adv. Space. Res. 49, 471–478.

Semones, E., IV-TEPC: status of the intravehicular – tissue equivalent proportional counter (IV-TEPC) development for ISS. In: The Sixteenth WRMISS Workshop took Place on 6–8 September 2011 in Prague, Czech Republic.

Shiragai, A., Noda, Y., Kumamoto, Y., Sato, Y., Murakami, T., 1998. Radiation protection for heavy ion therapy at NIRS-HIMAC II, 1998. In: Annual Report of the Research Project with Heavy Ions at NIRS-HIMAC II, NIRS-M-133, HIMAC-023, pp. 201–202.

Straube, U., Berger, T., Reitz, G., Facius, R., Fuglesang, C., Reiter, T., Damann, V., Tognini, M., 2010. Operational radiation protection for astronauts and cosmonauts and correlated activities of ESA medical operations. Acta. Astronaut. 66, 963–973.

Tawara, H., Doke, T., Hayashia, T., Kikuchi, J., Kyan, A., Nagaoka, S., Nakano, T., Takahashi, S., Terasawa, K., Yoshihira, E., 2002. LET distributions from CR-39 plates on Space Shuttle missions STS-84 and STS-91 and a comparison of the results of the CR-39 plates with those of RRMD-II and RRMD-III telescopes. Radiat. Meas. 35, 119–126.

Tawara, H., Masukawa, M., Nagamatsu, A., Kitajo, K., Kumagai, H., Yasuda, N., 2008. Measurement of a Linear Energy Transfer distribution with antioxidant doped CR-39 correcting for the dip angle dependence of track formation sensitivity. Jpn. J. Appl. Phys. 47, 7324–7327.

Tawara, H., Masukawa, M., Nagamatsu, A., Kitajo, K., Kumagai, H., Yasuda, N., 2011. Characteristics of Mg_2SiO_4:Tb (TLD-MSO) relevant for space radiation dosimetry. Radiat. Meas. 46, 709–716.

Yasuda, H., Fujitaka, K., 2000. Response of TLD-Mg_2SiO_4:Tb and radiophotoluminescent glass to heavy charged particles and space radiation. Radiat. Prot. Dosimetry. 87, 115–119.

Yasuda, N., Namiki, K., Honma, Y., Umeshima, Y., Marumo, Y., Ishii, H., Benton, E.R., 2005. Development of a high-speed imaging microscope and new software for nuclear track detector analysis. Radiat. Meas. 40, 311–315.

Zhou, D., Semones, E., Gaza, R., Johnson, S., Zapp, N., Weyland, M., 2007. Radiation measured for ISS-Expedition 12 with different dosimeters. Nucl. Instrum. Methods. Phys. Res. A. 580, 1283–1289.

Zhou, D., O'Sullivan, D., Semones, E., Zapp, N., Johnson, S., Weyland, M., 2008. Radiation dosimetry for high LET particles in low Earth orbit. Acta. Astronaut. 63, 855–864.